

Synthesis, in-silico based virtual screening, anti-cancer potential of novel 1,2,3-triazole-thiadiazole hybrid derivatives as Aurora kinase A (ARK-A) and Extracellular regulated kinase 2 (ERK2) dual inhibitors.

Lingaiah Bontha

Osmania University

Praveen Kumar E

Osmania University

Appaji Dokala

University of Hyderabad

Divya Pingili

Sri Venkateswara College of Pharmacy

Venkat Reddy Putta

Osmania University

Ravi kumar Vuradi

Osmania University

Laxma Reddy Kotha

Osmania University

sirasani Satyanarayana (✉ ssnsirasani@gmail.com)

osmania university

Research Article

Keywords: 1,2,3-triazole, thiadiazole, Anticancer activity, ARK-A/ERK, Dual inhibitors

Posted Date: March 23rd, 2023

DOI: <https://doi.org/10.21203/rs.3.rs-2691747/v1>

License: © ⓘ This work is licensed under a Creative Commons Attribution 4.0 International License.

[Read Full License](#)

Version of Record: A version of this preprint was published at Medicinal Chemistry Research on September 12th, 2023. See the published version at <https://doi.org/10.1007/s00044-023-03132-9>.

Abstract

As part of our ongoing efforts to produce promising cytotoxic agents, the novel compounds, 5-(4-(diethylamino)-2-((1-substitutedphenyl-1H-1,2,3-triazol-4-yl)methoxy)phenyl)-1,3,4-thiadiazol-2-yl)pyrrolidine-2,5-dione derivatives (9a-l) were developed, synthesised, and characterized using several analytical techniques, including ^1H NMR, ^{13}C NMR, and LC-MS. New series of 1,2,3-triazole and thiadiazole molecular hybrids synthesized were evaluated for their anticancer activity against human oesophageal carcinoma cell line KYSE-450 and human pancreatic carcinoma cell line MIA PaCa-2 cells. The compounds **9b**, **9i**, **9j**, and **9l** exhibited potential cytotoxic activity against KYSE-450 and MIA PaCa-2 cells, according to cytotoxic evaluation data. Compound **9j** had greater anti-cancer potential relative to the standard employed across all compounds evaluated. The remaining compounds exhibited moderate to weak anti-proliferative potential. *In-vitro* kinase inhibition of compound **9j** was significantly more effective against both ARK-1 and ERK-2 enzymes, indicating its dual inhibition potential. Docking analysis culminated that **9k**, **9j**, and **9i** have substantial docking scores with the ARK-1 receptor, indicating the presence of strong binding affinities. Significant binding interactions between molecules **9j** and **9h** and the ERK-2 receptor suggest an inhibitory effect. Hence the compounds are promising dual inhibitors of ARK-A/ERK2.

Introduction

Cancer is one of the most dangerous and life-threatening diseases in the world. It is the second-greatest cause of death around the globe.¹ According to WHO figures, by 2030, there would be 25 million new cases of cancer and 10 million deaths, with breast, lung, colon, rectum, and prostate cancers being the most prevalent.^{2,3} In this regard, cancer continues to pose a substantial risk to human health and a formidable obstacle to medical research in terms of the development of novel and effective anticancer medications.

Triazoles five-membered nitrogen heterocycles having three nitrogen and two carbon atoms in a ring. Triazoles are found to be effective bioisosteres of amides in bioactive molecules with diverse and important biological properties.⁴⁻⁷ 1,2,3-Triazole systems the ability of hydrogen bond formation, dipole-dipole and π stacking interactions, stable to reduction and oxidation.⁸ 1,2,3-triazoles are present in many of the drugs like the Tazobactam, Carboxyamidotriazole and Rufinamide etc. The triazoles are reported to have the anticancer^{9,10}, antitubercular¹¹, antifungal^{12,13} antibacterial^{14,15}, antiviral^{16,17} and antiobesity^{18,19} and anti-diabetic²⁰ properties.

Thiadiazole are the five membered heterocycles with two nitrogen atoms and a sulphur atom at 1,3 and 4 positions and an amine group at the 2nd position of the five membered ring. The 2-aminothiadiazoles are present in many of the drugs like the acetazolamide, megazol, cefazolin etc. The thiadiazole amines are reported to be having diverse biological activities like CA inhibition²¹, antibacterial²², antifungal²³,

anticancer^{24,25}, antileishmanial²⁶, anticonvulsant²⁷. The anticancer activities of the 1,2,3-triazole and tetrazole scaffolds (Fig. 1) motivates us to develop a hybrid with a good anticancer activity.

Taking into account the intriguing features of both triazole, tetrazole and thiadiazole mentioned in the literature we have designed and synthesized a new series of twelve 1,2,3-triazole- thiadiazole hybrid derivatives falling under the general formula shown in Fig. 1. The synthesized compounds were evaluated for cytotoxicity and apoptotic features to determine their anti-cancer potential against human oesophageal squamous cell carcinoma cells KYSE-450 having Arora kinase 1 (ARK-1) overexpression and pancreatic carcinoma cell line MIA PaCa-2 having ERK2 overexpression (MIAPaCa-2). The most promising derivatives of the series were then tested for *in-vitro* kinase inhibition potentials against ARK-1 and ERK2 dual inhibitory activity.

Results And Discussion

2.1 Chemistry: The synthetic route for the desired 1-(5-(4-(diethylamino)-2-((1-phenyl-1H-1,2,3-triazol-4-yl)methoxy)phenyl)-1,3,4-thiadiazol-2-yl)pyrrolidine-2,5-dione (9a-l) is summarized in scheme 1. The intermediate compound of 2-(5-amino-1,3,4-thiadiazol-2-yl)-5-(diethylamino)phenol (3) obtained from 4-(diethylamino)-2-hydroxybenzaldehyde (1) was reacted with thiosemicarbazide (5) in presence of TBHP in ethanol at room temperature for 4 hrs yielded 2-(5-amino-1,3,4-thiadiazol-2-yl)-5-(diethylamino)phenol (3). The compound (3) amine protection with succinic anhydride (4) in water reflux for 2.5 hrs and rt for overnight to obtain N-protected compound of 1-(5-(4-(diethylamino)-2-hydroxyphenyl)-1,3,4-thiadiazol-2-yl)pyrrolidine-2,5-dione (5). Free hydroxyl group containing compound (5) was then propargylated using propargyl bromide (6) in the presence of dry K₂CO₃ in dry DMF to give 1-(5-(4-(diethylamino)-2-(prop-2-ynyloxy)phenyl)-1,3,4-thiadiazol-2-yl)pyrrolidine-2,5-dione (7). The compound (7) on further reaction with substituted aryl azides (8a-l) to the formation of triazoles using click reaction to yield 1-(5-(4-(diethylamino)-2-((1-phenyl-1H-1,2,3-triazol-4-yl)methoxy)phenyl)-1,3,4-thiadiazol-2-yl)pyrrolidine-2,5-dione derivatives (9a-l). The products were obtained in yields (60–70%).

Cytotoxic evaluation

The newly synthesized hybrid molecules (**9a-l**) were screened for Human esophageal squamous cell carcinoma cell line KYSE-450 with ARK1 overexpression, pancreatic carcinoma cell line MIAPaCa-2 with ERK2 overexpression by using doxorubicin as standard drug. The calculated IC₅₀ values of all compounds presented in Table-3. The compounds **9b**, **9i** and **9j** showed superior activity against human esophageal carcinoma cell line KYSE-450 cell line with IC₅₀ values of 25.51 ± 1.38, 25.39 ± 1.35 and 23.74 ± 1.39 μM respectively, than the standard drug doxorubicin. Among the above three molecules listed, compound **9j** showed lowest IC₅₀ indicate substantial cytotoxic effects against KYSE-450 cells. On the other hand, compounds **9j**, and **9i** showed promising cytotoxic activity against human pancreatic cancer cell line MIA PaCa-2 cells with IC₅₀ of 20.62 ± 2.18, and 19.17 ± 1.16 μM respectively. Both the compounds reported for superior cytotoxic behaviour against MIA PaCa-2 cells. Remaining all other compounds were

failed to report significant effect on growth and proliferation of both KYSE-450 and MIA PaCa-2 cells. So these results demonstrated that compound **9j** showed dual inhibition of ARK-1 and ERK2 with substantial activity (Table 1 and Fig. 2). The activity of compounds **9b**, **9i**, **9j** and **9l** may be accredited to the presence of weak electron withdrawing group p-bromo, the electron donating function p-methoxy, p-methyl and m-acetyl weak electron withdrawing function in meta and para position.

Table 1
Anticancer activity of the synthesized compounds (**9a-l**).

Compound Code	Ic ₅₀ in μ M	
	KYSE-450	MIA PaCa-2
9a	41.23 \pm 1.4	36.59 \pm 3.86
9b	25.51 \pm 1.38	29.08 \pm 2.04
9c	35.69 \pm 1.76	33.13 \pm 2.86
9d	50.17 \pm 2.16	42.39 \pm 3.04
9e	68.17 \pm 3.25	41.75 \pm 2.49
9f	30.60 \pm 2.08	28.28 \pm 2.29
9g	59.63 \pm 4.63	40.16 \pm 2.74
9h	74.31 \pm 5.82	59.13 \pm 3.91
9i	25.39 \pm 1.35	22.93 \pm 1.67
9j	23.74 \pm 1.39	20.62 \pm 2.18
9k	65.03 \pm 6.08	62.17 \pm 025
9l	46.28 \pm 121.	19.17 \pm 1.16
Doxorubicin	27.06 \pm 2.84	21.31 \pm 0.83

Morphological observation

By observing morphological changes in KYSE-450 and MIA PaCa-2 cells, the cytotoxic effects of potent compounds (**9b**, **9i**, **9j**, and **9l**) were determined. Compounds with cytotoxic effects exhibited typical shared characteristics, including cell shrinkage, membrane rounding, nuclear condensation, and the production of vesicular structures in cells. These characteristic, typical morphological alterations in cytotoxic cells were commonly employed for the identification of morphological changes over the course of therapy. Hence, an inverted phase contrast microscope was employed to visualize the morphological alterations. Compared to control cells, KYSE-450 and MIA PaCa-2 cells exhibited morphological changes

after 24 hours of treatment with test chemicals (Fig. 3). Visualization of the control cells revealed that they retained their original morphology and architecture. In contrast, KYSE-450 and MIA PaCa-2 cells exposed to selected chemicals for 24 hours exhibited normal cellular deformation characteristics, including rounding, shrinkage, and loss of contact with neighboring cells. Compound **9j** had a significant effect on both KYSE-450 and MIA PaCa-2 cells, causing cellular morphological deformation. Compounds **9b** and **9i** manifested prominent effect on the cellular morphology of KYSE-450 cells, while compound **9l** had the same effect on MIA PaCa cells.

Dual kinase inhibition assay

The purpose of our developed compounds is to enhance ARK1/ERK2 dual inhibition and decrease toxicity. Thus, ARK1/ERK2 kinase inhibition was utilized to evaluate *in-vitro* enzymatic inhibitory investigations that ultimately reflect the tumor-inhibiting properties of developed drugs. The ARK1/ERK2 kinase inhibition experiment was conducted per the commercial assay developers' directions. As demonstrated in Table 4, only one (**9j**) among the twelve synthesized compounds exhibited high inhibitory activity against both ARK-1 and ERK2, indicating that the logical design of the molecule's chemistry contributed to its activity. Compound **9j** of the series displayed greater inhibition of both ARK1/ERK2 inhibitory actions, with respective IC₅₀ values of 0.018 ± 0.13 and 0.017 ± 0.124 μM. Compound **9b** displayed strong inhibitory action against ARK-1 with an IC₅₀ of 0.034 ± 0.166 μM, whereas **9l** revealed significant activity against ERK-2 with an IC₅₀ of 0.024 ± 0.192 μM. These results also corroborated the cytotoxic behaviour of these compounds indicated by their anti-proliferative properties.

Table 2. Kinase inhibition of compounds 9a-l.

Entry	Kinase inhibition in IC ₅₀ (μM)	
	ARK1	ERK2
9a	>1	>1
9b	0.034 ± 0.166	0.256 ± 0.134
9c	0.749 ± 0.133	0.698 ± 0.135
9d	0.481 ± 0.095	0.593 ± 0.104
9e	0.251 ± 0.007	0.459 ± 0.115
9f	0.547 ± 0.096	0.689 ± 0.108
9g	0.531 ± 0.003	0.028 ± 0.002
9h	0.813 ± 0.159	0.782 ± 0.186
9i	0.124 ± 0.166	0.024 ± 0.192
9j	0.018 ± 0.135	0.017 ± 0.124
9k	0.486 ± 0.116	0.509 ± 0.137
9l	0.047 ± 0.007	0.031 ± 0.003
Barasertib	0.021 ± 0.007	-
Temuterkib	-	0.019 ± 0.003

Molecular Docking with Aurora related kinase 1:

All of the ligand compounds have higher binding energies with Aurora kinase 1 (PDB ID: 1MQ4) than the standard reference Doxorubicin. The docking scores of compounds **9a-l** range from - 9.8 to -10.5 Kcal/mol, which is more than the value of -9.8 Kcal/mol for Doxorubicin (Table 3). CASTp server determined that the active site pocket of Aurora kinase 1 had the amino acids Leu139, Gly140, Lys141, Gly142, Lys143, Val147, Ala160, Lys162, His176, Arg180, Leu194, Glu211, Ala213 Thr217, Arg255, Glu260, Asn261, Leu263, Asn277, Trp277, Ser284, Arg285 and Thr. The new ligand molecules have also exhibited important interactions with the Aurora kinase1 active sites Lys141, Lys143, Lys162, Gln177, Ala213, Asp256, Asn261, Asp277, and Trp277. Compound **9k** exhibited the highest binding affinity of -10.5 Kcal/mol. It exhibited prominent interactions with Lys141, Lys162, and Ala213, as well as hydrophobic interactions with Leu139, Lys143, Phe144, Val147, Lys162, Glu181, Leu263, and Asp274 of 1MQ4 (Fig. 1,2). Compounds **9i** and **9j** had the second-highest binding affinity at -10.4 Kcal/mol. Compound **9i** defined key interactions with Asp256 and Asn261, while compound **9j** had significant interactions with Lys162, Asp256, and Asn261. Figure 2 depicts the H-bond and hydrophobic interactions of compounds **9i** and **9j**.

Table3. The binding energies and interactions of synthesized molecules with Aurora related kinase 1 (PDB ID: 1MQ4).

Compounds	Binding Energy (Kcal/mol)	Interacting amino acids	
		H-bond	hydrophobic
9a	-10.0	Lys143, Asp256, Asn261	Leu139, Val147, Ala160, Lys162, Ala213, Tyr219, Glu260, Leu263, Asp274
9b	-10.0	Asp256, Asn261, Trp277	Leu139, Lys143, Val147, Ala160, Lys162, Tyr212, Ala213, Leu263, Asp274
9c	-10.3	Asp256, Asn261, Trp277	Leu139, Lys143, Val147, Ala160, Lys162, Tyr212, Ala213, Leu263, Asp274
9d	-10.3	Asp256, Asn261, Trp277	Leu139, Lys143, Val147, Ala160, Lys162, Tyr212, Ala213, Leu263, Asp274
9e	-10.3	Lys143, Lys162, Asn261	Leu139, Lys141, Lys143, Val147, Ala160, Lys162, Ala213, Tyr219, Leu263, Asp274
9f	-9.8	Asp256, Glu260, Asn261, Trp277	Leu139, Lys143, Val147, Ala160, Lys258, Leu263, Asp274
9g	-9.9	Lys162, Gln177, Asp256, Asn261, Asp274	Leu139, Phe144, Val147, Ala160, Ala213, Asn261, Leu263, Asp277
9h	-10.2	Asp256, Glu260, Asn261, Asp274	Leu139, Lys143, Val147, Ala160, Glu260, Leu263, Asp274
9i	-10.4	Asp256, Asn261	Leu139, Lys143, Val147, Ala160, Lys162, Tyr212, Ala213, Leu263, Asp274, Trp277
9j	-10.4	Lys162, Asp256, Asn261	Leu139, Lys143, Val147, Ala160, Lys162, Ala213, Tyr219, Glu260, Leu263, Asp274
9k	-10.5	Lys141, Lys162, Ala213	Leu139, Lys143, Phe144, Val147, Lys162, Glu181, Leu263, Asp274
9l	-10.3	Ala213, Asp256, Asn261, Trp277	Leu139, Lys143, Val147, Ala160, Lys162, Leu263, Asp274
Doxorubicin	-9.8	Lys143, Glu260, Asn261, Asp274	Leu139, Lys141, Gly142, Val147, Ala160, Ala213, Leu263

Molecular docking with extracellular signal-related kinase 2 (ERK2):

The synthesized ligand molecules have scored best binding energies on par with standard reference Doxorubicin with ERK2 (PDB ID: 4ZXT). The docking scores of compounds 8a – 8l are ranging from – 8.2 to -9.3 Kcal/mol whereas Doxorubicin scored – 8.3 Kcal/mol. (Table 4). The active site pocket of ERK2 comprised of amino acids Ile31, Gly32, Glu33, Gly34, Ala35, Tyr36, Gly37, Met38, Val39, Ala52, Lys54, Lys55, Ile56, Arg67, Thr68, Glu71, Ile72, Leu75, Ile84, Ile103, Gln105, Asp106, Leu107, Met108, Glu109, Thr110, Asp111, Lys114, Asp149, Lys151, Ser153, Asn154, Leu156, Ile165, Asp167, Gly169 and Leu170 determined by CASTp server. The novel ligand molecules have also exhibited key interactions with active sites Glu33, Tyr39, Lys54, Arg67, Gln105, Met108, Asp111, Lys114, Ser153, and Asn154 of ERK2.

Table 4

The binding energies and interactions of synthesized molecules with extracellular signal-related kinase 2 (PDB ID: 4ZXT)

Compounds	Binding Energy (Kcal/mol)	Interacting amino acids	
		H-bond	hydrophobic
9a	-8.8	Gln105, Asp111, Lys114, Ser153	Ile31, Ala35, Tyr36, Val39, Ala52, Lys54, Ileu156, Asp167
9b	-8.3	Gln105, Asp111, Lys114, Ser153	Ile31, Ala35, Tyr36, Val39, Ala52, Lys54, Asp111, Lys114, Leu156, Asp167
9c	-8.2	Lys54, Asn154	Gly34, Ala35, Tyr36, Arg67, Ile84, Lys114, Leu156, Asp167
9d	-8.5	Gln105, Asp111, Lys114, Ser153	Ile31, Ala35, Tyr36, Val39, Ala52, Lys54, Asp111, Lys114, Asp167
9e	-8.8	Gln105, Asp111, Lys114, Ser153	Ala35, Tyr36, Val39, Ala52, Lys54, Asp111, Lys114, Leu156, Asp167
9f	-8.4	Asp111, Lys114, Ser153	Ile31, Ala35, Tyr36, Val39, Ala52, Lys54, Asp111, Lys114, Leu156, Asp167
9g	-8.2	Gln105, Asp111, Lys114, Ser153	Ile31, Ala35, Tyr36, Val39, Lys54, Asp111, Leu156, Asp167
9h	-9.0	Asp111, Lys114, Ser153	Ile31, Ala35, Tyr36, Val39, Lys54, Asp111, Lys114, Leu156, Asp167
9i	-8.5	Gln105, Asp111, Lys114, Ser153	Ile31, Ala35, Tyr36, Val39, Ala52, Lys54, Asp111, Lys114, Leu156, Asp167
9j	-9.3	Tyr39, Arg67, Lys151, Ser153, Asn154	Ala35, Val39, Lys54, Arg67, Lys151, Leu156, Asp167
9k	-8.2	Glu33, Met108, Asp111	Ile31, Val36, Val39, Ala52, Leu156
9l	-8.7	Gln105, Asp111, Lys114, Ser153	Ile31, Ala35, Tyr36, Val39, Ala52, Lys54, Asp111, Lys114, Leu156, Asp167
Doxorubicin	-8.3	Lys54, Gln105, Asp111, Lys114	Ile31, Gly34, Ala35, Tyr36, Asp111, Ser153, Asp167

Compound **9j** scored highest binding affinity value of -9.3 Kcal/mol. It exhibited H-bond interactions with Tyr39, Arg67, Lys151, Ser153, Asn154 and hydrophobic interaction with Ala35, Val39, Lys54, Arg67, Lys151, Leu156, Asp167 of ERK2 (Fig. 7,8). Compound **9h** scored second highest binding affinity value of -9.0 Kcal/mol. It defined key interactions with Asp111, Lys114, Ser153 and hydrophobic interactions with Ile31, Ala35, Tyr36, Val39, Lys54, Asp111, Lys114, Leu156, Asp167 of 4ZXT (Fig. 3).

Conclusion

A new series of molecular hybrids containing 1,2,3-triazole and thiazolidinediones were synthesized and evaluated for their anticancer activity against human oesophageal carcinoma cell lines KYSE-450 and human pancreatic carcinoma cell line MIA PaCa-2 cells. Docking studies revealed that **9k**, **9j**, and **9i** showed significant docking scores with ARK-1 receptor, indicated the strong binding interactions. Molecules **9j**, and **9h** exhibited significant binding interactions with ERK-2 receptor indicates inhibitory activity. Cytotoxic data examined that compounds **9b**, **9i**, **9j** and **9l** showed promising activity against KYSE-450 and MIAPaCa-2 cells. Among all compounds tested, compound **9j** showed superior anti-cancer potential compared to the standards used. The other compounds showed moderate to weak activities against the cell lines. Further Kinase inhibition of compound **9j** showed substantially higher effect against both ARK-1 and ERK-2 enzymes *in-vitro*. Concluding, the synthesized compounds are proved to be better lead compounds for the development of new anticancer agents.

Experimental

General experimental methods:

Unless specified all the chemicals and solvents were purchased from commercial vendors and used further purification. ^1H NMR and ^{13}C NMR spectra were recorded in DMSO by using 500 MHz spectrometers (BrukerAvance III 500 MHz). Chemical shift values are displayed as ppm and spin multiplicities are indicated as singlet (s); doublet (d); doublet of doublet (dd); triplet(t); multiplets (m); and coupling constants are shown in hertz. Column chromatography was performed on silica gel (60–120 mesh) using distilled hexane and ethyl acetate solvents. Mass and Infrared spectra were recorded on QSTAR XL GCMS, Perkin Elmer spectrum2 mass spectrometer. Melting points were determined in open glass capillary tube on a Stuart MP2. Melting Point apparatus and were uncorrected.

Synthesis of 2-(5-amino-1,3,4-thiadiazol-2-yl)-5-(diethylamino)phenol (**3**)

The 4-(diethylamino)-2-hydroxybenzaldehyde (**1**) in ethanol was added with thiosemicarbazide (**2**) at rt and stirred for 2 h then the reaction was cooled to 0–5°C and TBHP was added slowly to the reaction under inert conditions and then the reaction is continued stirring for another 35 h. after the TLC marked the completion of the reaction the solvent was evaporated and the residue was added with crushed ice and extracted 3x100 ml Ethyl acetate and dried over anhydrous sodium sulfate and evaporated under reduced pressure to afford 2-(5-amino-1,3,4-thiadiazol-2-yl)-5-(diethylamino)phenol (**3**) with 60% yield.

Synthesis of 1-(5-(4-(diethylamino)-2-hydroxyphenyl)-1,3,4-thiadiazol-2-yl)pyrrolidine-2,5-dione (**5**)

2-(5-amino-1,3,4-thiadiazol-2-yl)-5-(diethylamino)phenol (**3**) the amine protection with succinic anhydride (**4**) in water reflux for 2.5 hrs and rt for overnight to obtained 1-(5-(4-(diethylamino)-2-hydroxyphenyl)-1,3,4-thiadiazol-2-yl)pyrrolidine-2,5-dione (**5**)

Synthesis of 1-(5-(4-(diethylamino)-2-(prop-2-ynyloxy)phenyl)-1,3,4-thiadiazol-2-yl)pyrrolidine-2,5-dione (**6**)

A solution of compound (**6**) and dry K_2CO_3 in dry DMF at rt propargyl bromide (**7**) was added and stirred for 4 hrs and the reaction was monitored using TLC after completion the reaction mixture was dumped into crushed ice and stirred vigorously, the precipitate formed was filtered to afford 1-(5-(4-(diethylamino)-2-(prop-2-ynyloxy)phenyl)-1,3,4-thiadiazol-2-yl)pyrrolidine-2,5-dione (**6**) subjected to column chromatography with ethyl acetate and hexane as eluent (4:6).

General procedure for synthesis of 1-(5-(4-(diethylamino)-2-((1-phenyl-1 H -1,2,3-triazol-4-yl)methoxy)phenyl)-1,3,4-thiadiazol-2-yl)pyrrolidine-2,5-dione hybrids (**9a-l**)

To a solution of compound (**7**) (0.1 mmol) and appropriate aryl azides (**8a-l**) (0.15 mmol) in DMF: H_2O was added $CuSO_4 \cdot 5H_2O$ (3mol%) with sodium ascorbate (5 mol%) and stirred at room temperature for 6–8 hours. The completion of the reaction was monitored by TLC. Upon completion of the reaction, mass was purified by column chromatography using hexane/ ethyl acetate (1:3) to afford titled compounds (**9a-l**) with good yields 60–70%.

Anticancer Activity

Cellular Cytotoxicity Assays

Esophageal squamous cell carcinoma with ARK1 overexpression (KYSE-450), Pancreatic carcinoma cell line with ERK2 overexpression (MIAPaCa-2) were provided by the Centre for Cellular and Molecular Biology (CCMB), Hyderabad, India. Cells were cultured in RPMI 1640 medium supplemented with 10% FBS, and Penicillin 100 U/mL and Streptomycin 100U/mL were added. Cell cultures were maintained in a humidified atmosphere of 5% CO_2 at 37°C. Cells were seeded at respective densities (2.5×10^4 /mL) in 96-well plates in a volume of 180 μL per well. After seeding 24 h, the medium was removed. The test compounds were dissolved in DMSO and diluted with a culture medium to different concentrations (the final concentration of DMSO was 0.1%). Then, 20 μL of the test compound solution (**9a-l**) was added in duplicates, and incubation continued for 48 h in a humidified atmosphere of 5% CO_2 at 37°C. 20 μL of methylthiazolyldiphenyl-tetrazolium bromide (MTT) was added to each well after removing the medium and incubated for an additional 3–4 h. The growth medium was replaced by 150 μL DMSO to solubilize the purple formazan crystals produced, and the absorbance was measured on a microplate reader at 570

nm. The compound IC₅₀ values were calculated using Graph Pad Prism 5.0. Data represented as mean ± SD from three independent experiments.

Morphological Observation Using Phase Contrast Microscopy

Observation of morphological changes of cytotoxic effect was performed according to the method with slight modifications. Briefly, 5×10^5 cells were incubated for 48 hours with or without selected compounds (**9b**, **9i**, **9j**, and **9l**) at concentrations of double the IC₅₀ in a 60 mm diameter tissue culture dishes. The medium was discarded and cells were washed once with PBS. The morphological changes of the cytotoxic effect over the treatment were observed using phase contrast inverted microscope (Leica DMI 3000B, Germany) at 200x magnifications.

Kinase inhibitory assays

Selectivity screening of newly synthesized compounds (**9a-l**) against aurora kinase 1 (ARK1) and extracellular regulated kinase 1 (ERK1) kinases was performed by using Promega ADP-Glo™ bioluminescent detection of kinase assay kit as per the manufacturer's guidelines. Two kinases ARK1 and ERK1 were used in multipoint dose-response experiments. The kinase and substrate strips were diluted in 45 µL of 5x kinase buffer solution and 7.5µL of 200µM ATP, respectively. Kinase reactions were performed using 1 µL of the compound solution at varying concentrations (0.05 µM – 50 µM), 3 µL of kinase working stock, and 3 µL of ATP/substrate working stock. After 1h incubation at room 28°C temperature, kinase activity was quantified using the ADP-Glo Kinase Assay (Promega Corporation, Madison, WI, USA). Kinase inhibition was quantified using a luminescence microplate spectrophotometer Infinite M1000 (Tecan, Groding, Austria). The concentration of the test compounds required to decrease the kinase activity by 50% was determined using ImageJ software and identified as the IC₅₀. This study measures the quantitative behavior of ARK1/ERK2 inhibition.

Molecular Docking Studies

Molecular docking is a reliable, cost-effective, and time-saving technique in the process of drug discovery.²⁸ AutodockVina of PyRx tool is an open-source software tool²⁹ used for performing docking studies. Autodockvina uses an empirical scoring function to calculate the binding affinity of the protein-ligand complex.³⁰ For a better understanding of the binding interactions between ligand molecules and target cancer cells, the crystal structure of the breast cancer drug target aurora-related kinase 1 (PDB ID: **1MQ4**)³¹ and lung cancer drug target extracellular signal-related kinase 2 (ERK2) (PDB ID: **4ZXT**)³² were retrieved from Protein Data Bank (www.rcsb.org). The proteins were prepared by using the Biovia

Discovery Studio software tool. Initially, water molecules were removed and polar hydrogens were added to macromolecule. The ligands were sketched by using Chems sketch tool (www.acdlabs.com) and saved in MDL file format. Both target and ligand molecules were loaded into PyRx tool. The energies of ligands were minimized and converted to PDBQT file format. The protein was chosen as a macromolecule. The active site pockets of target molecules were determined by CASTp online server.³³ The 3D grid box was set up in such a way to cover the active site pocket of the target molecule and docking simulations were performed. After docking, conformations were ranked according to their binding energy, and the confirmation with the lowest binding energy was considered as the best docking score. The docking results were visualized using PyMOL and Biovia Discovery Studio Visualizer.

Spectral data:

2-(5-(4-(diethylamino)-2-((1-phenyl-1H-1,2,3-triazol-4-yl)methoxy)phenyl)-1,3,4-thiadiazol-2-yl)cyclopentane-1,3-dione (9a) Yield 60%, mp: 124–126 °C ; Rf = 0.34 (EtOAc:n-Hexane 2:3); ¹H NMR (500 MHz, DMSO-*d*₆) δ 8.55 (s, 1H), 7.73 (d, *J* = 7.6 Hz, 1H), 7.59–7.53 (m, 2H), 7.52–7.44 (m, 2H), 7.42–7.35 (m, 1H), 6.78 (d, *J* = 2.3 Hz, 1H), 6.52 (s, 1H), 5.38 (s, 2H), 3.47 (q, *J* = 7.0 Hz, 4H), 2.71 (s, 4H), 1.12 (t, *J* = 7.0 Hz, 6H); ¹³C NMR (125 MHz, DMSO-*d*₆) δ 174.10, 157.78, 156.66, 153.41, 150.82, 146.25, 135.72, 129.36, 129.19, 126.91, 120.13, 119.15, 114.14, 106.52, 98.39, 58.57, 43.83, 28.14, 11.66. LC-MS [M + H]⁺; 502.59: Elemental analysis, Calculated, %: C₂₆H₂₆N₆O₃S: C, 62.13; H, 5.21; N, 16.72; Found %: C, 62.08; H, 5.16; N, 16.68;

2-(5-(2-((1-(4-bromophenyl)-1H-1,2,3-triazol-4-yl)methoxy)-4-(diethylamino)phenyl)-1,3,4-thiadiazol-2-yl)cyclopentane-1,3-dione (9b) Yield 63%, mp: 121–123 °C ; Rf = 0.42 (EtOAc:n-Hexane 2:3); ¹H NMR (500 MHz, DMSO-*d*₆) δ 8.55 (s, 1H), 7.73 (d, *J* = 7.6 Hz, 1H), 7.70–7.58 (m, 4H), 6.78 (d, *J* = 2.3 Hz, 1H), 6.52 (s, 1H), 5.38 (s, 2H), 3.47 (q, *J* = 7.0 Hz, 4H), 2.71 (s, 4H), 1.12 (t, *J* = 7.0 Hz, 6H); ¹³C NMR (125 MHz, DMSO-*d*₆) δ 174.14, 157.82, 156.70, 153.45, 150.86, 146.29, 134.53, 133.05, 129.23, 120.91, 119.22, 119.06, 114.18, 106.56, 98.43, 58.61, 43.87, 28.18, 11.70: LC-MS [M + H]⁺; 581.48 Elemental analysis, Calculated, %: C₂₆H₂₅BrN₆O₃S: C, 53.70; H, 4.33; N, 14.45; Found %: C, 53.67; H, 4.31; N, 14.41

2-(5-(2-((1-(2-chlorophenyl)-1H-1,2,3-triazol-4-yl)methoxy)-4-(diethylamino)phenyl)-1,3,4-thiadiazol-2-yl)cyclopentane-1,3-dione(9c) Yield 61%, mp: 127–129 °C ; Rf = 0.40 (EtOAc:n-Hexane 2:3); ¹H NMR (500 MHz, DMSO-*d*₆) δ 8.46 (s, 1H), 7.79–7.71 (m, 2H), 7.52–7.44 (m, 2H), 7.37 (dd, *J* = 7.0, 1.3 Hz, 1H), 6.78 (d, *J* = 2.3 Hz, 1H), 6.52 (s, 1H), 5.37 (s, 2H), 3.47 (q, *J* = 7.0 Hz, 4H), 2.71 (s, 4H), 1.12 (t, *J* = 7.0 Hz, 6H); ¹³C NMR (125 MHz, DMSO-*d*₆) δ 174.13, 157.81, 156.69, 153.44, 150.85, 145.82, 135.02, 130.96, 129.22, 128.19, 127.53, 127.13, 120.42, 119.22, 114.17, 106.55, 98.42, 58.77, 43.86, 28.17, 11.69. LC-MS [M + H]⁺; 537.03: Elemental analysis, Calculated, %: C₂₆H₂₅ClN₆O₃S: C, 58.15; H, 4.69; N, 15.65; Found %: C, 58.11; H, 4.64; N, 15.61;

2-(5-(2-((1-(4-chlorophenyl)-1H-1,2,3-triazol-4-yl)methoxy)-4-(diethylamino)phenyl)-1,3,4-thiadiazol-2-yl)cyclopentane-1,3-dione(9d) Yield 65%, mp: 129–131 °C ; Rf = 0.40 (EtOAc:n-Hexane 2:3); ¹H NMR (500 MHz, DMSO-*d*₆) δ 8.55 (s, 1H), 7.76–7.70 (m, 3H), 7.48–7.42 (m, 2H), 6.78 (d, *J* = 2.3 Hz, 1H), 6.52 (s, 1H), 5.38 (s, 2H), 3.47 (q, *J* = 7.0 Hz, 4H), 2.71 (s, 4H), 1.12 (t, *J* = 7.0 Hz, 6H); ¹³C NMR (125 MHz, DMSO-*d*₆) δ 174.10, 157.78, 156.66, 153.41, 150.82, 146.25, 134.17, 134.06, 129.65, 129.19, 121.52, 119.14, 114.14, 106.52, 98.39, 58.57, 43.83, 28.14, 11.66. LC-MS [M + H]⁺; 537.03 Elemental analysis, Calculated, %: C₂₆H₂₅ClN₆O₃S: C, 58.15; H, 4.69; N, 15.65; Found %: C, 58.11; H, 4.64; N, 15.61;

2-(5-(4-(diethylamino)-2-((1-(4-hydroxyphenyl)-1H-1,2,3-triazol-4-yl)methoxy)phenyl)-1,3,4-thiadiazol-2-yl)cyclopentane-1,3-dione(9e) Yield 60%, mp: 127–129 °C ; Rf = 0.30 (EtOAc:n-Hexane 2:3); ¹H NMR (500 MHz, DMSO-*d*₆) δ 9.12 (s, 1H), 8.54 (s, 1H), 7.76–7.66 (m, 3H), 6.97–6.90 (m, 2H), 6.78 (d, *J* = 2.3 Hz, 1H), 6.52 (s, 1H), 5.38 (s, 2H), 3.47 (q, *J* = 7.0 Hz, 4H), 2.71 (s, 4H), 1.12 (t, *J* = 7.0 Hz, 6H); ¹³C NMR (125 MHz, DMSO-*d*₆) δ 174.14, 157.82, 156.70, 156.14, 153.45, 150.86, 146.28, 129.23, 129.00, 121.41, 119.55, 116.77, 114.18, 106.56, 98.43, 58.61, 43.87, 28.18, 11.70. LC-MS [M + H]⁺; 518.59: Elemental analysis, Calculated, %: C₂₆H₂₆N₆O₄S: C, 60.22; H, 5.05; N, 16.21; Found %: C, 60.18; H, 5.01; N, 16.17;

2-(5-(4-(diethylamino)-2-((1-(2-methoxyphenyl)-1H-1,2,3-triazol-4-yl)methoxy)phenyl)-1,3,4-thiadiazol-2-yl)cyclopentane-1,3-dione(9f) Yield 62%, mp: 121–123 °C ; Rf = 0.44 (EtOAc:n-Hexane 2:3); ¹H NMR (500 MHz, DMSO-*d*₆) δ 8.44 (s, 1H), 7.76–7.69 (m, 2H), 7.40 (dd, *J* = 7.1, 1.1 Hz, 1H), 7.18 (dd, *J* = 7.1, 1.4 Hz, 1H), 7.05 (d, *J* = 1.3 Hz, 1H), 6.78 (d, *J* = 2.3 Hz, 1H), 6.52 (s, 1H), 5.38 (s, 2H), 3.84 (s, 3H), 3.47 (q, *J* = 7.0 Hz, 6H), 2.71 (s, 4H), 1.12 (t, *J* = 7.0 Hz, 6H); ¹³C NMR (125 MHz, DMSO-*d*₆) δ 174.12, 157.80, 156.68, 153.43, 153.19, 150.84, 145.26, 129.21, 127.97, 126.20, 124.21, 119.25, 119.06, 114.16, 113.38, 106.54, 98.41, 58.76, 55.06, 43.85, 28.16, 11.68. LC-MS [M + H]⁺; 532.61: Elemental analysis, Calculated,%: C₂₇H₂₈N₆O₄S: C, 60.89; H, 5.30; N, 15.78; Found %: C, 60.84; H, 5.26; N, 15.73;

2-(5-(4-(diethylamino)-2-((1-(4-methoxyphenyl)-1H-1,2,3-triazol-4-yl)methoxy)phenyl)-1,3,4-thiadiazol-2-yl)cyclopentane-1,3-dione(9g) Yield 67%, mp: 126–128 °C ; Rf = 0.44 (EtOAc:n-Hexane 2:3); ¹H NMR (500 MHz, DMSO-*d*₆) δ 8.53 (s, 1H), 7.73 (d, *J* = 7.6 Hz, 1H), 7.66–7.59 (m, 2H), 7.06–6.99 (m, 2H), 6.78 (d, *J* = 2.3 Hz, 1H), 6.52 (s, 1H), 5.38 (s, 2H), 3.76 (s, 3H), 3.47 (q, *J* = 7.0 Hz, 6H), 2.71 (s, 4H), 1.12 (t, *J* = 7.0 Hz, 6H); ¹³C NMR (125 MHz, DMSO-*d*₆) δ 174.06, 159.15, 157.74, 156.62, 153.37, 150.78, 146.20, 130.05, 129.15, 121.39, 119.47, 114.62, 114.10, 106.48, 98.35, 58.53, 54.62, 43.79, 28.10, 11.62: LC-MS [M + H]⁺; 532. Elemental analysis, Calculated,%: C₂₇H₂₈N₆O₄S: C, 60.89; H, 5.30; N, 15.78; Found %: C, 60.84; H, 5.26; N, 15.73;

2-(5-(4-(diethylamino)-2-((1-(*o*-tolyl)-1H-1,2,3-triazol-4-yl)methoxy)phenyl)-1,3,4-thiadiazol-2-yl)cyclopentane-1,3-dione(9h) Yield 61%, mp: 119–121 °C ; Rf = 0.45 (EtOAc:n-Hexane 2:3); ¹H NMR (500 MHz, DMSO-*d*₆) δ 8.57 (s, 1H), 7.73 (d, *J* = 7.6 Hz, 1H), 7.69 (d, *J* = 1.4 Hz, 1H), 7.41 (dd, *J* = 7.1, 1.4 Hz, 1H), 7.29–7.19 (m, 2H), 6.78 (d, *J* = 2.3 Hz, 1H), 6.52 (s, 1H), 5.38 (s, 2H), 3.47 (q, *J* = 7.0 Hz, 6H), 2.71 (s, 4H), 2.32 (s, 3H), 1.12 (t, *J* = 7.0 Hz, 6H); ¹³C NMR (125 MHz, DMSO-*d*₆) δ 174.12, 157.80, 156.68, 153.43,

150.84, 145.86, 135.89, 132.10, 130.34, 129.21, 127.92, 126.79, 119.97, 119.08, 114.16, 106.54, 98.41, 58.76, 43.85, 28.16, 16.84, 11.68. LC-MS [M + H]⁺; 516.61: Elemental analysis, Calculated, %: C₂₇H₂₈N₆O₃S: C, 62.77; H, 5.46; N, 16.27; Found %: C, 62.73; H, 5.42; N, 16.24;

2-(5-(4-(diethylamino)-2-((1-(p-tolyl)-1H-1,2,3-triazol-4-yl)methoxy)phenyl)-1,3,4-thiadiazol-2-yl)cyclopentane-1,3-dione(9i) Yield 64%, mp: 124–126 °C; Rf = 0.47 (EtOAc:n-Hexane 2:3); ¹H NMR (500 MHz, DMSO-*d*₆) δ 8.54 (s, 1H), 7.73 (d, *J* = 7.6 Hz, 1H), 7.67–7.61 (m, 2H), 7.29–7.23 (m, 2H), 6.78 (d, *J* = 2.3 Hz, 1H), 6.52 (s, 1H), 5.38 (s, 2H), 3.47 (q, *J* = 7.0 Hz, 6H), 2.71 (s, 4H), 2.36 (s, 3H), 1.12 (t, *J* = 7.0 Hz, 6H); ¹³C NMR (125 MHz, DMSO-*d*₆) δ 174.12, 157.80, 156.68, 153.43, 150.84, 146.27, 136.51, 133.96, 129.87, 129.21, 119.65, 119.24, 114.16, 106.54, 98.41, 58.59, 43.85, 28.16, 20.41, 11.68. LC-MS [M + H]⁺; 516.61: Elemental analysis, Calculated, %: C₂₇H₂₈N₆O₃S: C, 62.77; H, 5.46; N, 16.27; Found %: C, 62.73; H, 5.42; N, 16.24;

2-(5-(2-((1-(3-acetylphenyl)-1H-1,2,3-triazol-4-yl)methoxy)-4-(diethylamino)phenyl)-1,3,4-thiadiazol-2-yl)cyclopentane-1,3-dione(9j) Yield 63%, mp: 127–129 °C; Rf = 0.35 (EtOAc:n-Hexane 2:3); ¹H NMR (500 MHz, DMSO-*d*₆) δ 8.64 (s, 1H), 8.15 (s, 1H), 7.83 (d, *J* = 1.3 Hz, 1H), 7.73 (d, *J* = 7.6 Hz, 1H), 7.68 (d, *J* = 1.4 Hz, 1H), 7.59 (dd, *J* = 7.3, 7.3 Hz, 1H), 6.78 (d, *J* = 2.3 Hz, 1H), 6.52 (s, 1H), 5.38 (s, 2H), 3.47 (q, *J* = 7.0 Hz, 4H), 2.71 (s, 4H), 2.62 (s, 3H), 1.12 (t, *J* = 7.0 Hz, 6H); ¹³C NMR (125 MHz, DMSO-*d*₆) δ 196.85, 174.14, 157.82, 156.70, 153.45, 150.86, 146.37, 137.58, 137.05, 129.23, 129.20, 125.54, 121.49, 119.02, 118.80, 114.18, 106.56, 98.43, 58.61, 43.87, 28.18, 26.06, 11.70. LC-MS [M + H]⁺; 544.62: Elemental analysis, Calculated, %: C₂₈H₂₈N₆O₄S: C, 61.75; H, 5.18; N, 15.43; Found %: C, 61.71; H, 5.14; N, 15.41;

2-(5-(2-((1-(4-acetylphenyl)-1H-1,2,3-triazol-4-yl)methoxy)-4-(diethylamino)phenyl)-1,3,4-thiadiazol-2-yl)cyclopentane-1,3-dione(9k) Yield 68%, mp: 131–133 °C; Rf = 0.34 (EtOAc:n-Hexane 2:3); ¹H NMR (500 MHz, DMSO-*d*₆) δ 8.59 (s, 1H), 7.95–7.89 (m, 2H), 7.77–7.71 (m, 3H), 6.78 (d, *J* = 2.3 Hz, 1H), 6.52 (s, 1H), 5.38 (s, 2H), 3.47 (q, *J* = 7.0 Hz, 4H), 2.71 (s, 4H), 2.56 (s, 3H), 1.12 (t, *J* = 7.0 Hz, 6H); ¹³C NMR (125 MHz, DMSO-*d*₆) δ 196.05, 174.08, 157.76, 156.64, 153.39, 150.80, 146.23, 137.51, 134.71, 129.90, 129.17, 119.36, 119.16, 114.12, 106.50, 98.37, 58.55, 43.81, 28.12, 25.70, 11.64. LC-MS [M + H]⁺; 544.62: Elemental analysis, Calculated, %: C₂₈H₂₈N₆O₄S: C, 61.75; H, 5.18; N, 15.43; Found %: C, 61.71; H, 5.14; N, 15.41;

2-(5-(4-(diethylamino)-2-((1-(4-nitrophenyl)-1H-1,2,3-triazol-4-yl)methoxy)phenyl)-1,3,4-thiadiazol-2-yl)cyclopentane-1,3-dione(9l) Yield 70%, mp: 137–139 °C; Rf = 0.34 (EtOAc:n-Hexane 2:3); ¹H NMR (500 MHz, DMSO-*d*₆) δ 8.57 (s, 1H), 8.37–8.30 (m, 2H), 7.97–7.90 (m, 2H), 7.73 (d, *J* = 7.6 Hz, 1H), 6.78 (d, *J* = 2.3 Hz, 1H), 6.52 (s, 1H), 5.38 (s, 2H), 3.47 (q, *J* = 7.0 Hz, 4H), 2.71 (s, 4H), 1.12 (t, *J* = 7.0 Hz, 6H); ¹³C NMR (125 MHz, DMSO-*d*₆) δ 174.10, 157.78, 156.66, 153.41, 150.82, 148.94, 146.32, 138.89, 129.19, 125.32, 120.52, 119.66, 114.14, 106.52, 98.39, 58.57, 43.83, 28.14, 11.66. LC-MS [M + H]⁺; 547.59: Elemental analysis, Calculated, %: C₂₆H₂₅N₇O₅S: C, 57.03; H, 4.60; N, 17.91; Found %: C, 56.98; H, 4.56; N, 17.87;

Declarations

Acknowledgments

All the authors are thankful to the Head, Department of chemistry, Osmania University, Hyderabad for providing laboratory facilities. We thank Central Facilities and Research Development (CFRD) analytical team for providing spectral analytical facilities.

Conflict of interest:

The authors declare no conflict of interest

References

1. Popova, E. A.; Protas, A. V.; Trifonov, R. E. Tetrazole Derivatives as Promising Anticancer Agents. *ACAMC***2018**, *17*(14). <https://doi.org/10.2174/1871520617666170327143148>.
2. Siegel, R. L.; Miller, K. D.; Fuchs, H. E.; Jemal, A. Cancer Statistics, 2022. *CA: A Cancer Journal for Clinicians***2022**, *72* (1), 7–33. <https://doi.org/10.3322/caac.21708>.
3. *Cancer*. <https://www.who.int/news-room/fact-sheets/detail/cancer> (accessed 2022-04-22).
4. Sahoo, S. K.; Ahmad, M. N.; Kaul, G.; Nanduri, S.; Dasgupta, A.; Chopra, S.; Yaddanapudi, V. M. Synthesis and Evaluation of Triazole Congeners of Nitro-Benzothiazinones Potentially Active against Drug Resistant Mycobacterium Tuberculosis Demonstrating Bactericidal Efficacy. *RSC Med. Chem.***2022**, *13* (5), 585–593. <https://doi.org/10.1039/D1MD00387A>.
5. Gour, J.; Gatadi, S.; Pooladanda, V.; Ghouse, S. M.; Malasala, S.; Madhavi, Y. V.; Godugu, C.; Nanduri, S. Facile Synthesis of 1,2,3-Triazole-Fused Indolo- and Pyrrolo[1,4]Diazepines, DNA-Binding and Evaluation of Their Anticancer Activity. *Bioorganic Chemistry***2019**, *93*, 103306. <https://doi.org/10.1016/j.bioorg.2019.103306>.
6. Stacy, D. M.; Le Quement, S. T.; Hansen, C. L.; Clausen, J. W.; Tolker-Nielsen, T.; Brummond, J. W.; Givskov, M.; Nielsen, T. E.; Blackwell, H. E. Synthesis and Biological Evaluation of Triazole-Containing N-Acyl Homoserine Lactones as Quorum Sensing Modulators. *Org. Biomol. Chem.***2013**, *11* (6), 938–954. <https://doi.org/10.1039/C2OB27155A>.
7. Zuo, Z.; Liu, X.; Qian, X.; Zeng, T.; Sang, N.; Liu, H.; Zhou, Y.; Tao, L.; Zhou, X.; Su, N.; Yu, Y.; Chen, Q.; Luo, Y.; Zhao, Y. Bifunctional Naphtho[2,3-*d*][1,2,3]Triazole-4,9-Dione Compounds Exhibit Antitumor Effects In Vitro and In Vivo by Inhibiting Dihydroorotate Dehydrogenase and Inducing Reactive Oxygen Species Production. *J. Med. Chem.***2020**, *63* (14), 7633–7652. <https://doi.org/10.1021/acs.jmedchem.0c00512>.
8. Mohammed, J. H.; Mohammed, A. I.; Abass, S. J. Antibacterial Activity Importance of 1, 2, 3-Triazole and 1, 2, 4-Triazole by Click Chemistry. **2015**, 8.
9. Mareddy, J.; Nallapati, S. B.; Anireddy, J.; Devi, Y. P.; Mangamoori, L. N.; Kapavarapu, R.; Pal, S. Synthesis and Biological Evaluation of Nimesulide Based New Class of Triazole Derivatives as

- Potential PDE4B Inhibitors against Cancer Cells. *Bioorganic & Medicinal Chemistry Letters***2013**, *23* (24), 6721–6727. <https://doi.org/10.1016/j.bmcl.2013.10.035>.
10. Kumbhare, R. M.; Dadmal, T. L.; Ramaiah, M. J.; Kishore, K. S. V.; Pushpa Valli, S. N. C. V. L.; Tiwari, S. K.; Appalanaidu, K.; Rao, Y. K.; Bhadra, M. pal. Synthesis and Anticancer Evaluation of Novel Triazole Linked N-(Pyrimidin-2-Yl)Benzo[d]Thiazol-2-Amine Derivatives as Inhibitors of Cell Survival Proteins and Inducers of Apoptosis in MCF-7 Breast Cancer Cells. *Bioorganic & Medicinal Chemistry Letters***2015**, *25* (3), 654–658. <https://doi.org/10.1016/j.bmcl.2014.11.083>.
 11. Shaikh, M. H.; Subhedar, D. D.; Nawale, L.; Sarkar, D.; Khan, F. A. K.; Sangshetti, J. N.; Shingate, B. B. 1,2,3-Triazole Derivatives as Antitubercular Agents: Synthesis, Biological Evaluation and Molecular Docking Study. *Med. Chem. Commun.***2015**, *6* (6), 1104–1116. <https://doi.org/10.1039/C5MD00057B>.
 12. Pasko, M. T.; Piscitelli, S. C.; Van Slooten, A. D. Fluconazole: A New Triazole Antifungal Agent. *DICP***1990**, *24* (9), 860–867. <https://doi.org/10.1177/106002809002400914>.
 13. Lass-Flörl, C. Triazole Antifungal Agents in Invasive Fungal Infections. *Drugs***2011**, *71* (18), 2405–2419. <https://doi.org/10.2165/11596540-000000000-00000>.
 14. Bangalore, P. K.; Vagolu, S. K.; Bollikanda, R. K.; Veeragoni, D. K.; Choudante, P. C.; Misra, S.; Sriram, D.; Sridhar, B.; Kantevari, S. Usnic Acid Enaminone-Coupled 1,2,3-Triazoles as Antibacterial and Antitubercular Agents. *J. Nat. Prod.***2020**, *83* (1), 26–35. <https://doi.org/10.1021/acs.jnatprod.9b00475>.
 15. Aouad, M. R.; Mayaba, M. M.; Naqvi, A.; Bardaweel, S. K.; Al-blewi, F. F.; Messali, M.; Rezki, N. Design, Synthesis, in Silico and in Vitro Antimicrobial Screenings of Novel 1,2,4-Triazoles Carrying 1,2,3-Triazole Scaffold with Lipophilic Side Chain Tether. *Chemistry Central Journal***2017**, *11* (1), 117. <https://doi.org/10.1186/s13065-017-0347-4>.
 16. Głowacka, I. E.; Balzarini, J.; Wróblewski, A. E. Design, Synthesis, Antiviral, and Cytotoxic Evaluation of Novel Phosphonylated 1,2,3-Triazoles as Acyclic Nucleotide Analogues. *Nucleosides Nucleotides Nucleic Acids***2012**, *31* (4), 293–318. <https://doi.org/10.1080/15257770.2012.662611>.
 17. Alvarez, R.; Velázquez, S.; San-Félix, A.; Aquaro, S.; De Clercq, E.; Perno, C. F.; Karlsson, A.; Balzarini, J.; Camarasa, M. J. 1,2,3-Triazole-[2',5'-Bis-O-(Tert-Butyldimethylsilyl)-Beta-D- Ribofuranosyl]-3'-Spiro-5''-(4''-Amino-1'',2''-Oxathiole 2'',2''-Dioxide) (TSAO) Analogues: Synthesis and Anti-HIV-1 Activity. *J Med Chem***1994**, *37* (24), 4185–4194. <https://doi.org/10.1021/jm00050a015>.
 18. Poulsen, S.-A.; Wilkinson, B. L.; Innocenti, A.; Vullo, D.; Supuran, C. T. Inhibition of Human Mitochondrial Carbonic Anhydrases VA and VB with Para-(4-Phenyltriazole-1-Yl)-Benzenesulfonamide Derivatives. *Bioorganic & Medicinal Chemistry Letters***2008**, *18* (16), 4624–4627. <https://doi.org/10.1016/j.bmcl.2008.07.010>.
 19. Rajan, S.; Puri, S.; Kumar, D.; Babu, M. H.; Shankar, K.; Varshney, S.; Srivastava, A.; Gupta, A.; Reddy, M. S.; Gaikwad, A. N. Novel Indole and Triazole Based Hybrid Molecules Exhibit Potent Anti-Adipogenic and Antidyslipidemic Activity by Activating Wnt3a/β-Catenin Pathway. *European Journal of Medicinal Chemistry***2018**, *143*, 1345–1360. <https://doi.org/10.1016/j.ejmech.2017.10.034>.

20. Praveenkumar E, Nirmala Gurrapu, Prashanth Kumar Kolluri , Vishwanadham Yerragunta, Bharathi Reddy Kunduru , Subhashini N.J.P.Synthesis, anti-diabetic evaluation and molecular docking studies of 4-(1- aryl-1H-1, 2, 3-triazol-4-yl)-1,4- dihydropyridine derivatives as novel 11- β hydroxysteroid dehydrogenase-1 (11 β - HSD1) inhibitors. *Bioorganic Chemistry***2019** , 90, 103056.
<https://doi.org/10.1016/j.bioorg.2019.103056>
21. Supuran, C. T.; Scozzafava, A. Carbonic Anhydrase Inhibitors. *Current Medicinal Chemistry - Immunology, Endocrine & Metabolic Agents***2001**, 1 (1), 61–97.
<https://doi.org/10.2174/1568013013359131>.
22. Subhashini N.J.P, Praveen Kumar E, Nirmala Gurrapu , Vishwanadham Yerragunt. Design and synthesis of imidazolo-1, 2,3-triazoles hybrid compounds by microwave-assisted method: Evaluation as an antioxidant and antimicrobial agents and molecular docking studies. *Journal of Molecular Structure***2019** 1180, 618e628. <https://doi.org/10.1016/j.molstruc.2018.11.029>
23. Matysiak, J.; Malinski, Z. [2-(2,4-Dihydroxyphenyl)-1,3,4-thiadiazole analogues: antifungal activity in vitro against Candida species]. *Bioorg Khim***2007**, 33 (6), 640–647.
<https://doi.org/10.1134/s1068162007060106>.
24. Matysiak, J.; Opolski, A. Synthesis and Antiproliferative Activity of N-Substituted 2-Amino-5-(2,4-Dihydroxyphenyl)-1,3,4-Thiadiazoles. *Bioorganic & Medicinal Chemistry***2006**, 14 (13), 4483–4489.
<https://doi.org/10.1016/j.bmc.2006.02.027>.
25. Rzeski, W.; Matysiak, J.; Kandefer-Szerszeń, M. Anticancer, Neuroprotective Activities and Computational Studies of 2-Amino-1,3,4-Thiadiazole Based Compound. *Bioorganic & Medicinal Chemistry***2007**, 15 (9), 3201–3207. <https://doi.org/10.1016/j.bmc.2007.02.041>.
26. Tahghighi, A.; Razmi, S.; Mahdavi, M.; Foroumadi, P.; Ardestani, S. K.; Emami, S.; Kobarfard, F.; Dastmalchi, S.; Shafiee, A.; Foroumadi, A. Synthesis and Anti-Leishmanial Activity of 5-(5-Nitrofuran-2-Yl)-1,3,4-Thiadiazol-2-Amines Containing N-[(1-Benzyl-1H-1,2,3-Triazol-4-Yl)Methyl] Moieties. *European Journal of Medicinal Chemistry***2012**, 50, 124–128.
<https://doi.org/10.1016/j.ejmech.2012.01.046>.
27. Rajak, H.; Singour, P.; Kharya, M. D.; Mishra, P. A Novel Series of 2,5-Disubstituted 1,3,4-Oxadiazoles: Synthesis and SAR Study for Their Anticonvulsant Activity. *Chem Biol Drug Des***2011**, 77 (2), 152–158. <https://doi.org/10.1111/j.1747-0285.2010.01066.x>.
28. Lu, Z.-H.; Gu, X.-J.; Shi, K.-Z.; Li, X.; Chen, D.-D.; Chen, L. Accessing Anti-Human Lung Tumor Cell Line (A549) Potential of Newer 3,5-Disubstituted Pyrazoline Analogs. *Arabian Journal of Chemistry***2017**, 10 (5), 624–630. <https://doi.org/10.1016/j.arabjc.2014.11.002>.
29. S, A. K.; Madderla, S.; Dharavath, R.; Nalaparaju, N.; Katta, R.; Gundu, S.; Thumma, V.; B, P.; D, A. Microwave Assisted Synthesis of N-Substituted Acridine-1,8-Dione Derivatives: Evaluation of Antimicrobial Activity. *Journal of Heterocyclic Chemistry***2022**, 59 (7), 1180–1190.
<https://doi.org/10.1002/jhet.4458>.
30. Abdulfatai, U.; Uzairu, A.; Uba, S. Molecular Docking and Quantitative Structure-Activity Relationship Study of Anticonvulsant Activity of Aminobenzothiazole Derivatives. *Beni-Suef University Journal of*

- Basic and Applied Sciences***2018**, 7(2), 204–214. <https://doi.org/10.1016/j.bjbas.2017.11.002>.
31. Trott, O.; Olson, A. J. AutoDock Vina: Improving the Speed and Accuracy of Docking with a New Scoring Function, Efficient Optimization, and Multithreading. *J. Comput. Chem.***2009**, NA-NA. <https://doi.org/10.1002/jcc.21334>.
32. Nowakowski, J.; Cronin, C. N.; McRee, D. E.; Knuth, M. W.; Nelson, C. G.; Pavletich, N. P.; Rogers, J.; Sang, B.-C.; Scheibe, D. N.; Swanson, R. V.; Thompson, D. A. Structures of the Cancer-Related Aurora-A, FAK, and EphA2 Protein Kinases from Nanovolume Crystallography. *Structure***2002**, 10(12), 1659–1667. [https://doi.org/10.1016/S0969-2126\(02\)00907-3](https://doi.org/10.1016/S0969-2126(02)00907-3).
33. Lim, D. Y.; Shin, S. H.; Lee, M.-H.; Malakhova, M.; Kurinov, I.; Wu, Q.; Xu, J.; Jiang, Y.; Dong, Z.; Liu, K.; Lee, K. Y.; Bae, K. B.; Choi, B. Y.; Deng, Y.; Bode, A.; Dong, Z. A Natural Small Molecule, Catechol, Induces c-Myc Degradation by Directly Targeting ERK2 in Lung Cancer. *Oncotarget***2016**, 7(23), 35001–35014. <https://doi.org/10.18632/oncotarget.9223>.
34. Tian, W.; Chen, C.; Lei, X.; Zhao, J.; Liang, J. CASTp 3.0: Computed Atlas of Surface Topography of Proteins. *Nucleic Acids Research***2018**, 46(W1), W363–W367. <https://doi.org/10.1093/nar/gky473>.

Scheme 1

Scheme 1 is available in Supplementary Files section.

Figures

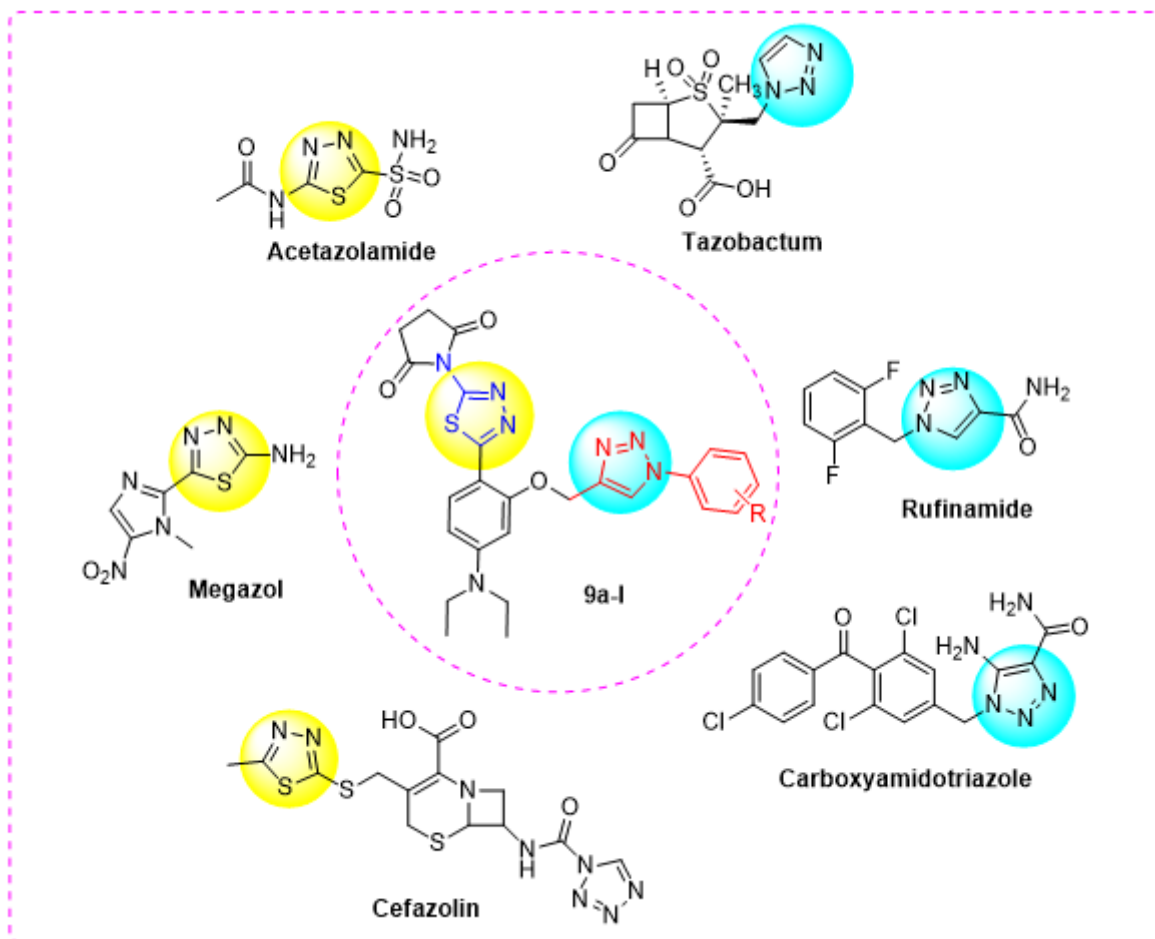


Figure 1

Design rationale for the 1,2,3-triazole-thiadiazolehybrids.

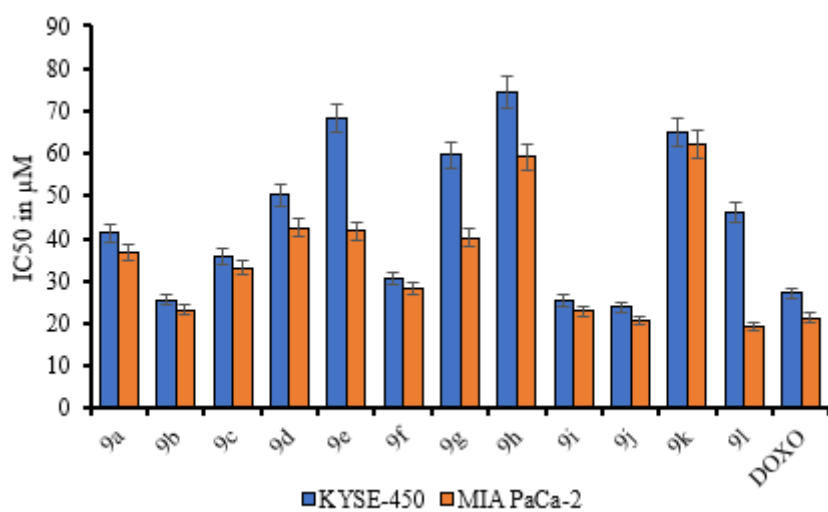


Figure 2

IC₅₀ of newly synthesized series (9a-l) against KYSE-450 and MIA PaCa cells.

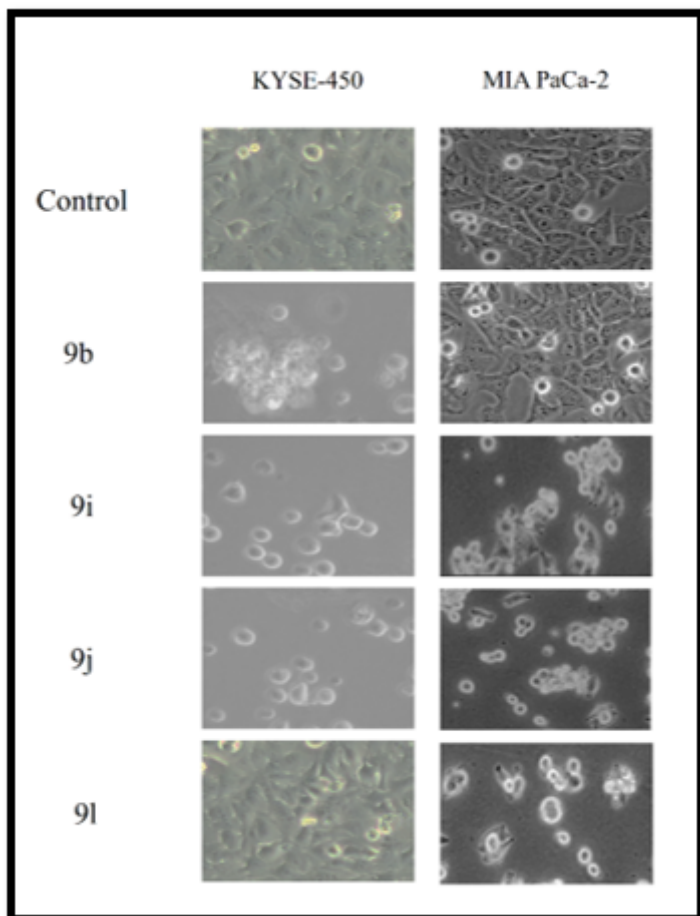


Figure 3

Morphological examination of selected compounds (9b, 9i, 9j, and 9l) against KYSE-450 and MIA PaCa-2 cells

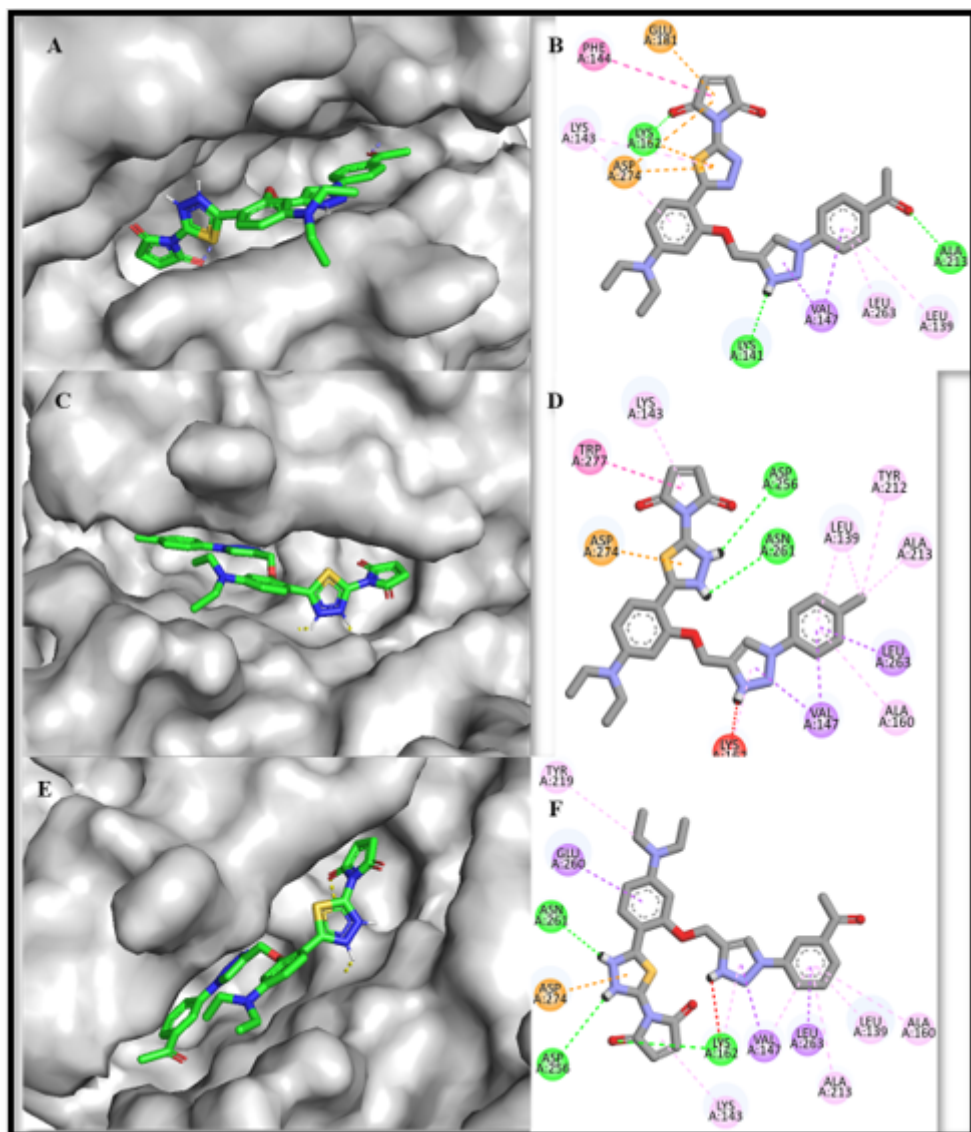


Figure 4

A) 3D and B) 2D Docking pose of compound 9k in cavity of 1MQ4; C) 3D and D) 2D Docking pose of compound 9i in cavity of 1MQ4; E) 3D and F) 2D Docking pose of compound 9j in cavity of 1MQ4.

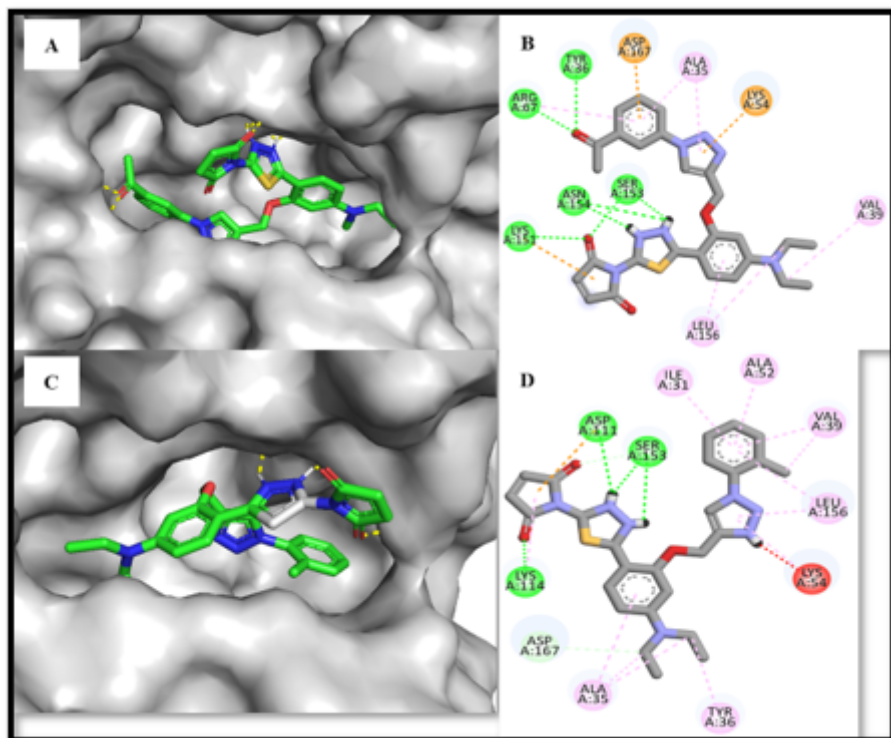


Figure 5

A) 3D and B) 2D Docking pose of compound **9j** in cavity of 4ZXT; C) 3D and D) 2D Docking pose of compound **9h** in cavity of 4ZXT.

Supplementary Files

This is a list of supplementary files associated with this preprint. Click to download.

- [Supplementaryfile.docx](#)
- [GraphicalAbstract.pptx](#)
- [Scheme1.png](#)